Photoacoustic in Situ Measurement of Quantum Efficiencies for Photoanodic Reactions at n-Type Semiconductor Electrodes

Sachio Yoshihara,* Ayyasamy Aruchamy, and Akira Fujishima
Department of Synthetic Chemistry, Faculty of Engineering, The University of Tokyo,
Hongo, Bunkyo-ku, Tokyo 113

(Received September 19, 1987)

Synopsis. The time required for the in situ measurement of quantum efficiencies during photoelectrochemical reactions is qreatly reduced by the photoacoustic spectroscopy (PAS) employing a piezoelectric transducer (PZT). PAS has been successfully applied for several reactions at TiO_2, ZnO, and CdS photoelectrodes and compared with previous studies by the photothermal spectroscopy (PTS).

In recent papers, we have reported on the measurement of quantum efficiencies during photoelectrochemical reactions by the photothermal spectroscopy (PTS).[1-4] In PTS, the heat produced during the relaxation of the excited carriers is detected as the change in the temperature of the semiconductor electrode. The advantage of this method is that the quantum efficiency determination does not require the calibration of the light source. But, PTS requires a longer measurement time because the time constant of the thermistor used as the sensor is quite large (ca. 1s). So, we had to measure the PT signal for various potentials fixing the electrode potential at each value. The slope of the straight line plot of PT signal vs. electrode potential gave the quantum efficiency. Therefore, it is of interest to utilize sensors having faster response.

In the present work, we have been able to measure quantum efficiencies within a very short time by the photoacoustic spectroscopy (PAS) employing a piezoelectric transducer (PZT). Since the time constant of the PZT employed is very small (approximately 0.1 μs), we considered that the experiment time may be significantly reduced. This method may also be developed for the investigation of certain relaxation processes during the photoelectrochemical reactions.

Experimental

Instrumental. The complete setup for this experiment is shown in Fig. 1. Either He–Cd laser (325 nm; CDR 80 SG. Kimmon Electric Company Limited) or Ar-ion laser (488 nm; Spectra Physics 164) was employed as the light source. The laser beam was chopped by a light chopper (8—800 Hz; CH-353. NF Circuit Design Block).

The cell was equipped with a platinum counter electrode and a saturated calomel reference electrode (SCE). The laser beam was transmitted into the cell through an optically flat window of the cell. A nitrogen bubbler was employed for deoxygenating the solutions.

The working electrodes were cadmium sulfide single crystal [(001) surface, Teikoku Tsushin Company Limited] which had dimensions $10\times10\times1\ \text{mm}^3$ and a carrier density of $4.8\times10^{16}\ \text{cm}^{-3}$, titanium dioxide prepared by firing Ti plate, and zinc oxide polycrystals [ZnO powder, ca. 1g (Wako Pure Chemical Industries) pressed at $150\ \text{kg cm}^{-2}$ and sintered at 1300 °C for 3 h] which had dimensions $15\phi\times1.5\ \text{mm}^3$. The ohmic contact was made by In–Ga alloy on one side of each crystal and then a copper wire was attached to the contact with silver paste. A piezoelectric transducer (NEPEC NPM, N 21 or N 6; $10\phi\times1\ \text{mm}^3$, Tohoku Metal Industries) was attached to the same side where the contact has been given after interposing thin epoxy resin layer. Finally, the whole of the electrode except the front surface was covered with epoxy resin. The structure of the semiconductor electrode (with a PZT in place) is shown in Fig. 2. The semiconductor surface was etched just before use in concentrated hydrochloric acid for 10 s.

The signal from the piezoelectric transducer was detected by a lock-in amplifier (LI-574, NF Circuit Design Block) and the current-potential curve was measured under potentiostatic conditions using a potentiostat (HF 301, Hokuto Denko Company Limited) and a potential programmer (NPS-2, Nikko Keisoku Company Limited). The cyclic voltammogram was displayed on an X-Y recorder (Type 3033, Yokogawa Electric Works).

All chemicals were of reagent grade and were used without further purification.

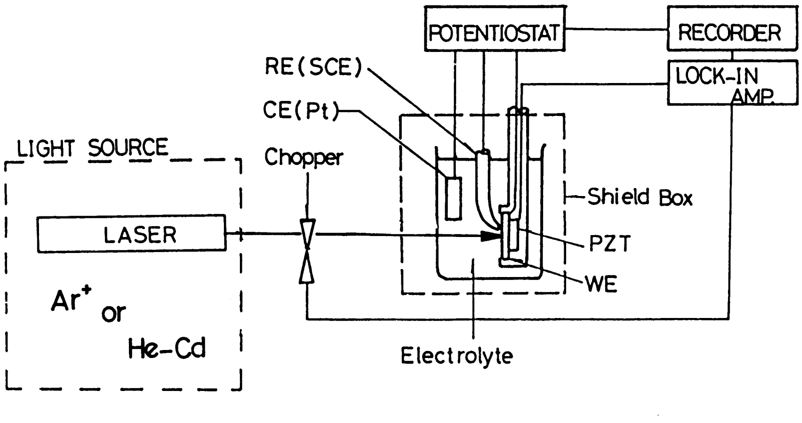

Fig. 1. Schematic diagram of the experimental setup for PAS.

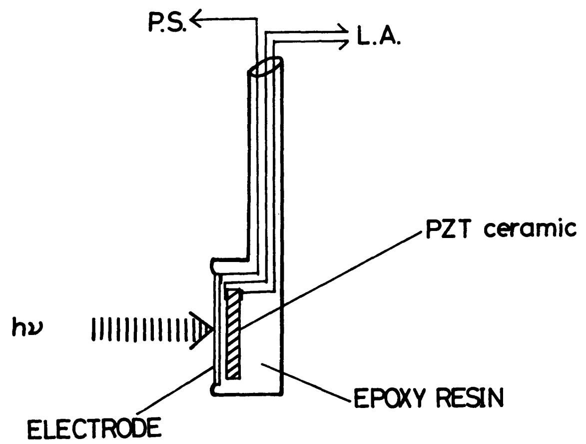

Fig. 2. Structure of the photoelectrode for PAS measurement.

Results and Discussion

The equation developed for the PTS[1] can be applied to the PAS also, since both mothods involve essentially the measurement of heat signals and the theoretical considerations are the same. For PAS the equation becomes

$$E(\Delta P/\Delta P_o) = (Q_{sc} + T\Delta S)/(It) + e\eta_q(V - V_{fb})$$

where E is the energy of the incident monochromatic light (eV/photon), I is the average absorbed intensity of light (photons/s), t is the illumination time (s), Q_{sc} is the heat evolved in the semiconductor via recombination and other radiationless processes, $T\Delta S$ is the heat evolved in term of an entropy change for the whole cell reaction (Electrochemical Peltier heat), e is elementary electric charge. η_q is the quantum efficiency of the photooxidation, ΔP and ΔP_0 are the PA signal amplitudes from the PZT at applied potential V and in the open circuit respectively, V_{fb} is the flatband potential.

Therefore, under constant illumination conditions (i.e. EIt held constant), a plot of $E(\Delta P/\Delta P_0)$ against $(V-V_{fb})$ yields the quantum efficiency, η_q, from the slope of the straight line.

The following semiconductor/electrolyte systems were investigated.

(1) n-TiO_2/Na_2SO_4, aq. ($4OH^- \rightarrow O_2+2H_2O+4e^-$)
(2) n-CdS/Na_2SO_4, Na_2SO_3aq. ($2SO_3^{2-}+2p^+ \rightarrow S_2O_6^{2-}$)[5–7]
(3) n-ZnO/Na_2SO_4 aq. ($2ZnO+4p^+ \rightarrow 2Zn^{2+}+O_2$)[8]
(4) n-TiO_2/Na_2SO_4, HCOONa aq. ($p^++HCOO^- \rightarrow CO_2+H^++e^-$; Current doubling)[9,10]
(5) n-CdS/Na_2SO_4, HCOONa aq. ($p^++HCOO^- \rightarrow CO_2+H^++e^-$; Current doubling)[11]
(6) n-ZnO/Na_2SO_4, HCOOH aq. ($ZnO+2p^++2HCOO^- \rightarrow Zn^{2+}+H_2O+2CO_2+2e^-$; Current doubling)[12–14]

Figure 3 shows the dependence of the photocurrent and the relative change in the PA signal ($\Delta P/\Delta P_0$) multiplied by the photon energy (E) on the electrode potential (V) for the CdS/Na_2SO_4, Na_2SO_3 aq. system. It is seen that the PA signal amplitude is proportional to the electrode potential in the saturated photocurrent region. Taking the slope equal to the quantum efficiency, we found that the η values measured by PAS in this study are in good agreement with those obtained by PTS.[1–4] (See Tables 1 and 2) We have already reported that the quantum efficiency obtained by PTS coincides with the one obtained by actinometry. The apparently large difference in the η values of TiO_2 in Tables 1 and 2 is due to the fact that a single crystal was used for the earlier PTS study whereas we used a polycrystalline TiO_2 prepared by thermal oxidation of Ti in the present study. It is also known that the thermally formed TiO_2 gives a higher quantum efficiency.[15,16]

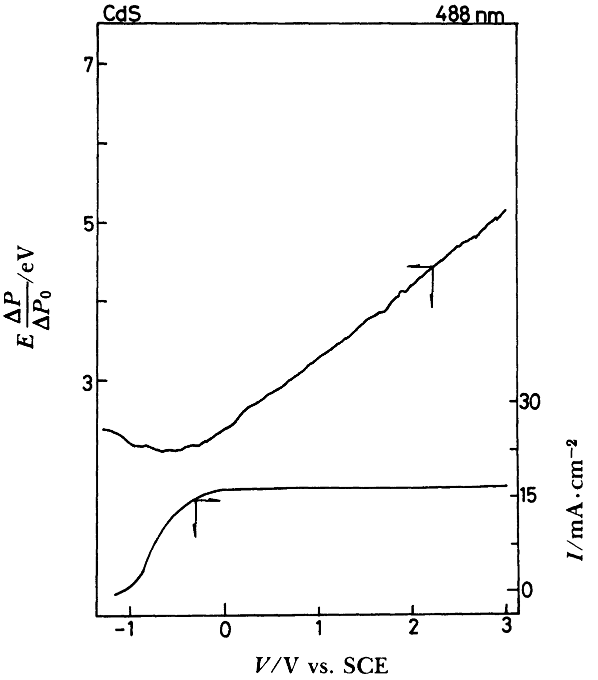

Fig. 3. Dependence of I (Photocurrent) and $E(\Delta P/\Delta P_0)$ on V (Applied potential) n-CdS Photoelectrode in 0.2 mol dm^{-3} Na_2SO_4, 1 mol dm^{-3} Na_2SO_3 aq. (Chopping frequency: 10 Hz).

The dependence of ΔP_0 and the quantum efficiency on the chopping frequency have also been measured in order to find out the optimum conditions for measurement. Since the signal is detected by the lock-in method, the magnitude of the PAS signal is expected to decrease exponentially and Fig. 4 shows such behavior. On the other hand, the quantum efficiency is almost independent of the frequency. However, η shows a larger scatter at high frequencies while the value appears to be precise at lower frequencies. This is because the quantum efficiency is determined from ΔP_0 and ΔP and the precision is greater when ΔP and ΔP_0 become larger. The signals are large in the lower frequency region. However at too low frequencies (<1 Hz), sensitivity of the PZT used decreases. Therefore, a moderate chopping frequency must be chosen for this experiment.

Table 1. Measured Quantum Efficiencies for n-TiO_2, n-CdS, and n-ZnO by Photoacoustic Spectroscopy, ( ) Stands for the Value in the Case of Current Doubling Reaction

	Saturation current[a)]	Quantum efficiency
	mA cm^{-2}	η
n-TiO_2[b)]	5.44 (6.24)	0.8±0.05 (1.0±0.05)
n-CdS	16.4 (28.0)	0.9±0.01 (1.5±0.01)
n-ZnO	2.72 (5.36)	0.8±0.1 (1.5±0.1)

a) For TiO_2 and ZnO relatively low powder He–Cd laser (325 nm) and for CdS high power Ar-ion laser (488 nm) were used. b) TiO_2 electrode was prepared by thermal oxidation of Ti metal plate.

Table 2. Measured Quantum Efficiencies for n-TiO_2, n-CdS, and n-ZnO by Photothermal Spectroscopy,[1–4)] ( ) Stands for the Value in the Case of Current Doubling Reaction

	Saturation current	Quantum efficiency
	mA cm^{-2}	η
n-TiO_2[a)]	1.63 (2.15)	0.6 (0.7)
n-CdS	0.85 (1.43)	1.0 (1.7)
n-ZnO	1.23 (2.25)	0.9 (1.8)

a) Single crystal TiO_2.

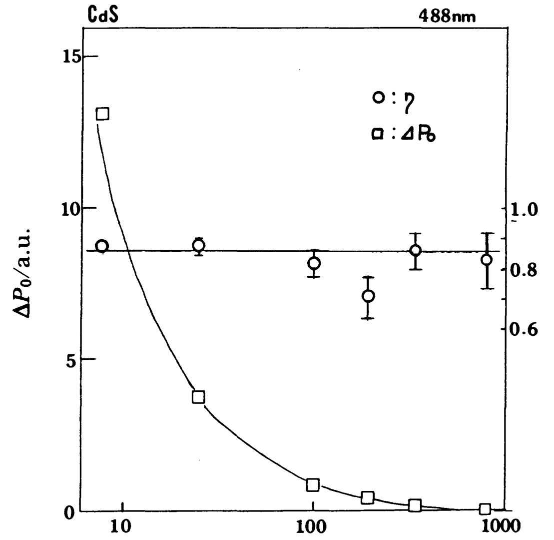

Fig. 4. Dependences of η (Quantum efficiency) and ΔP_0 (Photoacoustic signal amplitude at open circuit) on Chopping frequency, n-CdS Photoelectrode on 0.2 mol dm^{-3} Na_2SO_4, 1 mol dm^{-3} Na_2SO_3 aq.

Conclusion

In the PAS technique the Joule heat or the heat generated by the recombination of the excited carriers is detected as the distortion of the material or the acoustic wave from the material. This method requires much shorter time than the PTS for evaluating the quantum efficiency because of the very short time constant of the PZT. The efficiency values determined by PAS are in good agreement with PTS measurements. In future PAS utilizing PZT may be developed to obtain information concerning the recombination rates of photogenerated carriers by measuring the dependence of PA signal on the chopping frequency or the phase difference between PA signal and the reference signal. The recombination rates between CB and VB, the trapping rates of the photogenerated minority carriers at the surface recombination centers and the tunneling rates of electrons are some of the most important parameters in the semiconductor/electrolyte system. Work in this laboratory is under way to estimate above factors in the case of p-InP photoelectrodes.

We wish to thank Hisao Nakajima for his technical assistance and appreciate financial support from Ministry of Education, Science and Culture, Grant-in-Aid.

References

1) A. Fujishima, Y. Maeda, G. H. Brilmyer, and A. J. Bard, *J. Electrochem. Soc.*, **127**, 840 (1980).

2) Y. Maeda, A. Fujishima, and K. Honda, *Chem. Lett.*, **1980**, 271.

3) A. Fujishima, Y. Maeda, and K. Honda, *Bull. Chem. Soc. Jpn.*, **53**, 2735 (1980).

4) Y. Maeda, A. Fujishima, and K. Honda, *J. Electrochem. Soc.*, **128**, 1731 (1981).

5) T. Inoue, T. Watanabe, A. Fujishima, K. Honda, and K. Kohayakawa, *J. Electrochem. Soc.*, **124**, 719 (1977).

6) H. Gerischer and J. Gobrecht, *Ber. Bunsenges. Phys. Chem.*, **80**, 327 (1976).

7) H. Minoura and M. Tsuiki, *Electrochim. Acta.*, **23**, 1377 (1978).

8) H. Gerischer, *J. Electrochem. Soc.*, **113**, 1174 (1966).

9) V. A. Benderskii, Ya. M. Zolotovitskii, Ya. L. Kogan, M. L. Khidekel, and B. M. Shub, *Dokl. Akad. Nauk. SSSR*, **222**, 606 (1975).

10) M. Miyake, H. Yoneyama, and H. Tamura, *Chem. Lett.*, **1976**, 635.

11) H. Gerischer, *Surf. Sci.*, **18**, 97 (1969).

12) M. Morrison and T. Freund, *J. Chem. Phys.*, **47**, 1543 (1967).

13) S. R. Morrison and T. Freund, *Electrochim. Acta*, **13**, 1343 (1968).

14) W. P. Gomes, T. Freund, and S. R. Morrison, *J. Electrochem. Soc.*, **115**, 818 (1968).

15) E. C. Dutoit, F. Cardon, F. Vanderkerchove, and W. P. Gomes, *J. Appl. Electrochem.*, **8**, 247 (1978).

16) A. Aruchamy, Ph. D. Thesis, Indian Institute of Technology, Madras, India (1981).